CrossMark

Reactive wetting of alumina by Ti-rich Ni–Ti–Zr alloys

Peter Siegmund[1] · Conrad Guhl[1] · Elke Schmidt[2] · Andreas Roßberg[2] ·
Markus Rettenmayr[1]

Abstract Active brazing is a commonly used method for joining ceramic materials. In the present study, the wetting behavior of four Ti-rich ternary Ni–Ti–Zr alloys was investigated through sessile drop experiments on alumina disks of 96 and 99.9 % purity. The microstructure at the metal/alumina interface was analyzed using scanning electron microscopy and energy-dispersive X-ray spectroscopy. Three of the analyzed alloys exhibited reactive wetting with final contact angles between 40° and 70°. The reaction phases at the metal/alumina interface had a thickness of about 1 μm and were of a similar composition for all alloys. Dilatometer measurements showed thermal expansion coefficients between 13.2 and 15.8 × 10^{-6} °C^{-1}. The lowest wetting angle of 40° was achieved with the alloy 61Ti–20Zr–19Ni at temperatures above 980 °C.

Introduction

Most metals show limited or no wettability on ceramic substrates due to the differences in their chemical nature. Metals are therefore not suitable for joining ceramic materials [1]. Reactive brazing is a technique that relies on chemically active metals such as Ti, Zr, or V. Adding those elements to a brazing alloy can improve the wetting behavior of the liquid metal drastically and hence is a commonly used method for joining ceramic materials. The active element reacts with the ceramic substrate and thus creates a solid bond.

The process of reactive wetting has been investigated by numerous authors. Eustathopoulos formulated the RPC (reaction product control) model [2]. He states that the formation of the reaction product is the most important factor for the kinetics of reactive wetting. He also investigated the wetting of different oxide ceramics with the same braze alloy and discovered the formation of identical reaction products [3]. Another model for reactive wetting was proposed by Saiz et al. [4, 5], where the process of reactive wetting is divided into four different stages. In this model, the adsorption of the reactive element at the interface and the formation and movement of a ridge at the triple line are the most important factors for the reaction kinetics. Gómez-García et al. discussed the influence of electrostatic forces and impurities on the wetting process [6]. A good overview over the state of the art of reactive wetting can be found in the review articles of Akselsen [7] and Kumar et al. [8].

The most common method to determine the behavior of such active brazing alloys is a wetting experiment. The temporal evolution of the contact angle is used to characterize the wetting characteristics. A low contact angle frequently correlates with a high joint strength after brazing

✉ Markus Rettenmayr
  m.rettenmayr@uni-jena.de

  Peter Siegmund
  peter.siegmund@uni-jena.de

  Conrad Guhl
  conrad.guhl@uni-jena.de

  Elke Schmidt
  elke.schmidt@pcm.endress.com

  Andreas Roßberg
  andreas.rossberg@pcm.endress.com

1 Chair of Metallic Materials, Otto Schott Institute of Materials Research, Friedrich Schiller University Jena, Löbdergraben 32, 07743 Jena, Germany

2 Endress+Hauser GmbH+Co. KG, Hauptstrasse 1, 79689 Maulburg, Germany

[7, 9, 10]. The reaction products formed at the metal–ceramic interface are often very brittle, which lowers the joint strength significantly. It is therefore desirable to achieve a reaction phase as thin as possible to minimize the probability of crack initiation and propagation at the interface.

One of the most commonly used alloys for active brazing is eutectic Ag–Cu with the addition of a small amount of Ti as active element. This alloy provides an excellent wetting behavior on alumina and offers high joint strengths, but exhibits little flexibility in adjusting the brazing temperature and interdiffusion kinetics to different processing conditions and is costly due to the content in noble metal. We were looking for an active braze that creates a strong joint with potential variability in the liquidus and brazing temperatures. Additionally it should have a lower thermal expansion coefficient than common Ag–Cu–Ti alloys. Suitable alloys for joining alumina were found in preliminary experiments in the Ni–Ti–Zr system. Ti and Zr have both been found to act as active elements in the wetting process. Ti is the most commonly used active element and is known to achieve favorable wetting behavior in various active braze alloys. It has the highest chemical activity of these elements, so a reaction of the alumina with Ni–Ti–Zr alloys containing a high amount of Ti is to be expected. As

substrate material, alumina as the most commonly used ceramic material with a wide range of technical applications was selected. Four ternary Ti-rich Ni–Ti–Zr alloy compositions were chosen and their suitability as active braze alloy for joining alumina was investigated in this study. The alloys were analyzed via wetting experiments on alumina and the microstructure at the metal/alumina interface was investigated by SEM analyses.

Materials and methods

The compositions of the tested alloys were selected based on the investigation of the Ni–Ti–Zr system by Gupta [11]. As can be seen in Fig. 1, the selected alloys are situated in the vicinity of the quasi-peritectic equilibria U1 and U4, ensuring liquidus temperatures below 950 °C (for liquidus temperature see Table 1). The following alloys were used for the experiments (all compositions in at%):

alloy A: 61Ti–20Zr–19Ni
alloy B: 53Ti–13Zr–34Ni
alloy C: 70Ti–5Zr–25Ni
alloy D: 64Ti–15Zr–21Ni.

Fig. 1 Partial liquidus projection of the Ni–Ti–Zr system in the composition region of 0 to 50 at.% Ni (adapted from [11]). The compositions of the tested alloys are marked with *A–D*
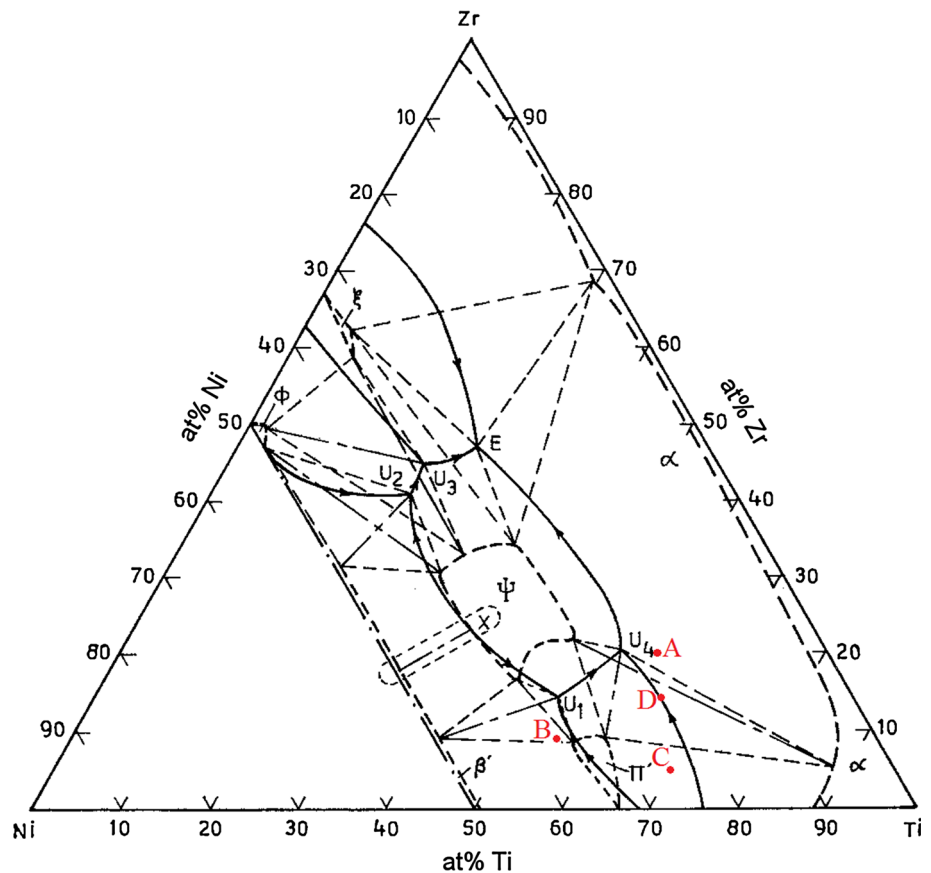
Table 1 Average final contact angles and liquidus temperatures of the analyzed alloys

Alloy	Mean final contact angle	Liquidus temperature (°C)
A: 61Ti–20Zr–19Ni ($T < 980$ °C)	60°	876
A: 61Ti–20Zr–19Ni ($T > 980$ °C)	40°	876
B: 53Ti–13Zr–34Ni	85°	927
C: 70Ti–5Zr–25Ni	65°	946
D: 64Ti–15Zr–22Ni	70°	849

Comparing the content of the active elements Ti and Zr in the alloy, we expect Ti to have a bigger influence on the wetting behavior since it has the higher electronegativity (1.54 compared to 1.33) and thus a higher chemical activity. The alloys were made using a cold wall crucible in an induction furnace. The set-up of the furnace allowed melting in levitation as a result of repulsive forces between the crucible and the alloy. The furnace was evacuated to a pressure of 5×10^{-5} mbar and flooded with Ar of 99.9990 % purity before melting. The temperature was measured using a pyrometer that was placed on a window on the top of the furnace. The liquidus temperatures were determined from a cooling curve that was recorded for each alloy. The starting materials for producing the alloys were obtained from E. Wagener GmbH in the form of rods and exhibited the following purities:

Ni 99.9 %
Ti 99.7 %
Zr 97.8 %, containing up to 2.0 % Hf

Hf is a common impurity in Zr, and it is tedious to separate it from the Zr due to its very similar properties. In most industrial applications Hf containing Zr is used. The effect of the Hf on the wetting and reaction behavior of the alloys was not further investigated. A significant influence of Hf is not to be expected. It is in the same subgroup in the periodic table of the elements and completely miscible with Zr. The highest Hf content was in alloy A with 0.4 at%. Neither liquidus temperature nor reaction behavior of the alloy at the interface should be changed significantly.

The alloys were cut with a diamond saw into pieces sized about 5 mm × 5 mm × 5 mm which resulted in a weight of the cubes between 0.6 and 0.75 g. The alloys were cleaned in an ultrasonic bath using acetone before the wetting experiments. The samples were placed on alumina disks of 96 and 99.9 % purity. The disks were put onto a graphite cylinder, which was inductively heated at its lower end in the same Ar-atmosphere as mentioned above. It was ensured that the metal alloy was well shielded from the induction field by the graphite. The samples were heated at a high rate; the experimental temperatures were reached after 2–3 min. The temperature was controlled by the pyrometer on top of the furnace. After the wetting experiments, the samples were cooled down to room temperature within ∼20 min. The development of the contact angle of the molten alloys was observed through a second window at the side of the furnace and monitored by a video camera. The recordings of the temperature and the video were started simultaneously to make the correlation of the wetting process and the temperature visible. The contact angles of the droplets were taken from single images extracted from the video files. Images were processed using the software ImageJ, and contact angles were measured manually by placing a tangent at the triple point of the droplet. The error of this method is about ±1°, as was ascertained through repeated measurements.

After the wetting experiments, the samples were cut using a diamond saw. The cross sections were ground with SiC paper and subsequently polished with 1 μm diamond paste. The polished samples were coated with carbon for electrical conductivity and examined in the scanning electron microscope (SEM) Leica S440i. The composition of the microstructure was analyzed with the energy-dispersive X-ray spectroscopy (EDX) unit Oxford EDX 5431 using a ZAF correction algorithm from the LINK/ISIS analysis software and employing the library standards provided by the manufacturer. The calibration was done with a Co standard of 99.99 % purity. The following relative errors of the EDX analysis were given by the manufacturer:

±1 % for concentrations >20 wt%
±5 % for concentrations between 10 and 20 wt%
±10 % for concentrations between 5 and 10 wt%
±50 % for concentrations <5 wt%

The coefficients of thermal expansion of the alloys were determined in the dilatometer DIL402E from Netzsch, considering that the difference in the coefficients of thermal expansion of the alloy and the ceramic is an important factor in the development of residual stresses during cooling in a brazing joint. For this, the alloys were cut into pieces sized 25 mm × 5 mm × 5 mm and heated from room temperature to 700 °C at a rate of 10 °C min^{-1}.

Results

Wetting angle measurements of Ni–Ti–Zr alloys on alumina

The wetting experiments showed similar results for the two different alumina substrate purities of 96 and 99.9 %. Thus, in the following analyses the compositions of alumina

Fig. 2 Droplet of the liquid braze alloy A on alumina, 200 s after melting

Fig. 3 Temporal evolution of the contact angle for different Ti–Ni–Zr alloys on alumina; the experimental temperatures depicted in the Figure were applied for overall 6 min without further changes of the contact angle

substrates will not be treated separately. The experiments were carried out at variable temperatures between 50 and 100 °C above the liquidus temperature of each alloy. A significant influence of different temperatures on the developing contact angle was only observed for alloy A. Figure 2 depicts a droplet of alloy C 200 s after melting, when the equilibrium contact angle was reached. For each of the alloys, the results of a representative experiment are shown in Fig. 3.

Due to the high reactivity of the alloys, the initial contact angles just after the melting of the alloys are hard to capture. Before the melting process was completed, a droplet had already formed and the process of reactive wetting had started. This involved an advancing triple line and a change in contact angle. After approximately 2 s, the alloys were completely liquid and the contact angles could be measured accurately.

As can be seen in Fig. 3, the initial contact angles were between 75° and 87° and decreased distinctly during the first seconds after melting. Given that the first reliable contact angle was obtained a few seconds after the melting started, it can be concluded that the initial contact angles were several degrees higher than depicted in Fig. 3. The rate of the decrease of the contact angles slowed down with increasing time. About 50–100 s after melting, the contact angles remained constant. The experiments were continued for another 5 min without a significant change in the shape of the droplets.

Each of the alloys showed a decrease of the contact angle during the wetting experiments, although to a different extent: the largest reduction of the contact angle (about 50°) was observed for alloy A when tested at temperatures above 980 °C. At lower temperatures, the alloy showed a similar behavior for the first 10 s, and then the contact angle remained stable at ~60°. The spreading of the droplets of alloy B stopped a few seconds after melting after a decrease of the contact angle of about 5°–10°. The average final contact angles and the liquidus temperatures of each alloy are summarized in Table 1.
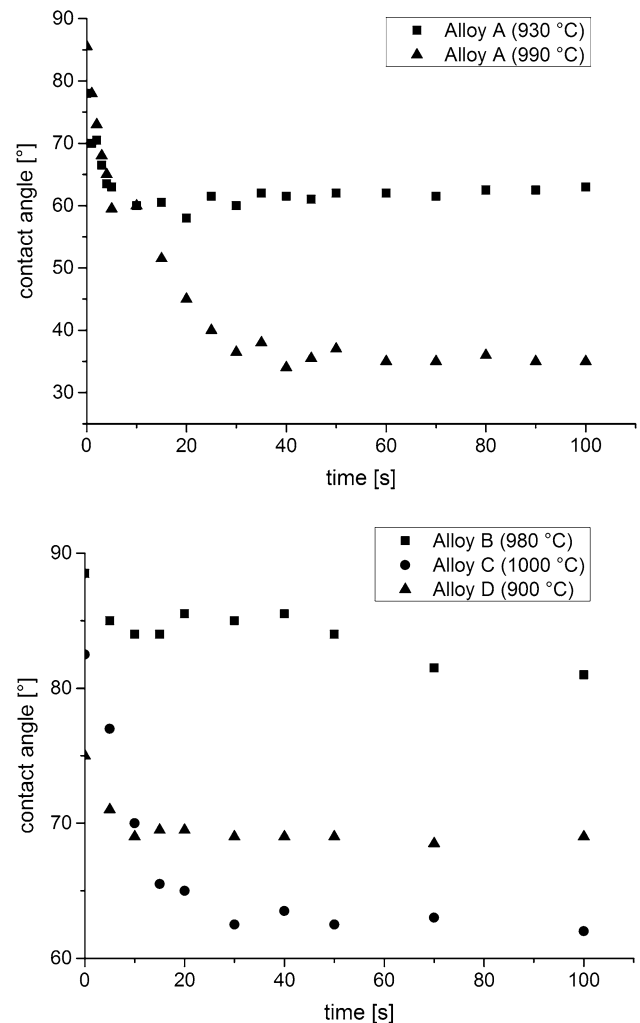
SEM analysis of the metal–alumina interface

After the wetting experiments, a cross section of each sample was analyzed using scanning electron microscopy (SEM) and energy-dispersive X-ray spectroscopy (EDX). Figure 4 shows the metal/alumina interface for all alloys. The microstructure of the alloys can be seen at the top part of the Figures while the alumina appears black at the bottom part. The different components of the microstructure in the vicinity of the interface are labeled with numbers and the mean compositions at the marked positions are listed in Table 2. These compositions (excluding the Al) are additionally marked in a section of the ternary Ni–Ti–Zr phase diagram (Fig. 5) to compare them with the phases stated by Gupta [11]. The properties of the known phases found in the cross sections of the wetting samples are listed in Table 3.
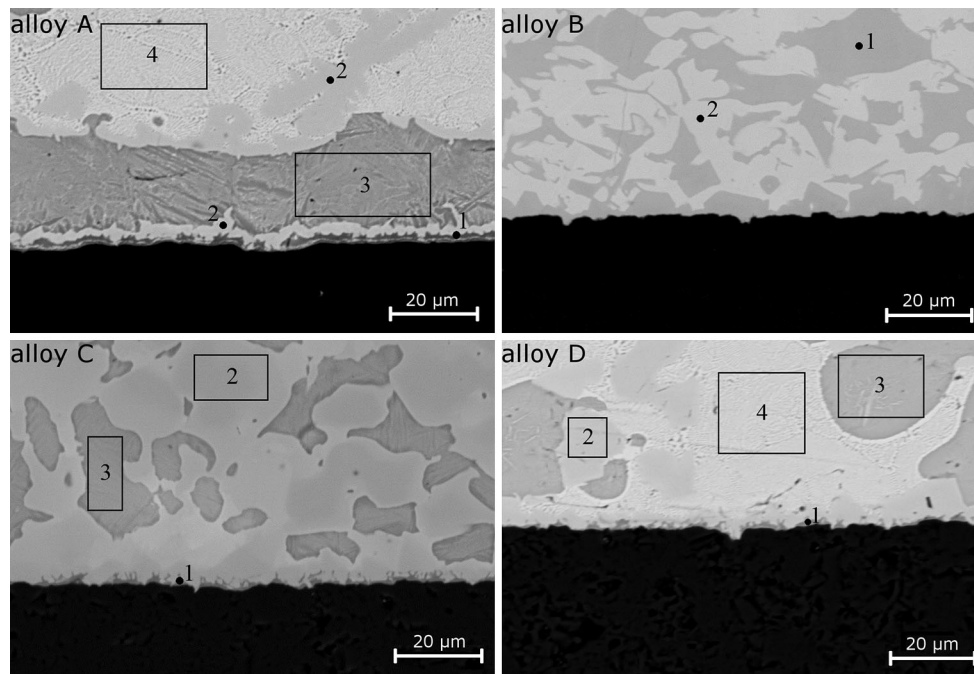
Fig. 4 SEM micrographs in the vicinity of the metal/alumina interface of the alloys *A–D*, all images were taken with an accelerating voltage of 20 kV in BSE mode

Table 2 EDX analysis of cross sections of the wetting samples: mean compositions of the marked areas of the microstructure (see Fig. 4) and assigned phases

Alloy	Position	Ni (at.%)	Ti (at.%)	Zr (at.%)	Al (at.%)	Phase according to composition
A	1	4	78	10	8	?
	2	28	56	16	–	?
	3	5	82	13	–	α (Ti, Zr)
	4	24	54	22	–	Peritectic (α + ψ)
B	1	35	47	18	–	ψ (NiTiZr)
	2	32	60	8	–	π′ (NiTi₂)
C	1	12	75	2	11	?
	2	32	65	3	–	π′ (NiTi₂)
	3	6	89	5	–	α (Ti, Zr)
D	1	4	74	5	17	?
	2	32	59	9	–	π′ (NiTi₂)
	3	6	85	9	–	α (Ti, Zr)
	4	24	59	17	–	Peritectic (α + ψ)

The microstructure of alloy A shown in Fig. 4 was only observed for temperatures above 980 °C. At lower temperatures, the microstructure did not contain the layer of the bright phase marked with number 2 at the interface. As depicted in Fig. 4, this phase also forms in small amounts at some positions above the layer of α (Ti, Zr) which is marked with number 3. The compositions of the observed phases were compared with the equilibrium phases as specified in the Ni–Ti–Zr phase diagram [11]. Most parts of the microstructure could be identified (see Table 2). With

the exception of alloy B, all samples exhibited at least one unknown phase at the metal/alumina interface. As can be seen in Fig. 5, all unknown phases are rich in Ti and are located near the α (Ti, Zr) phase. Each of the phases contains a significant amount of aluminum, which evidently is not depicted in the ternary phase diagram. It is therefore assumed that these phases do not belong to the α (Ti, Zr) phase, but are the result of a chemical reaction between metal and alumina. It is likely that they contain a significant amount of oxygen. However, a quantitative
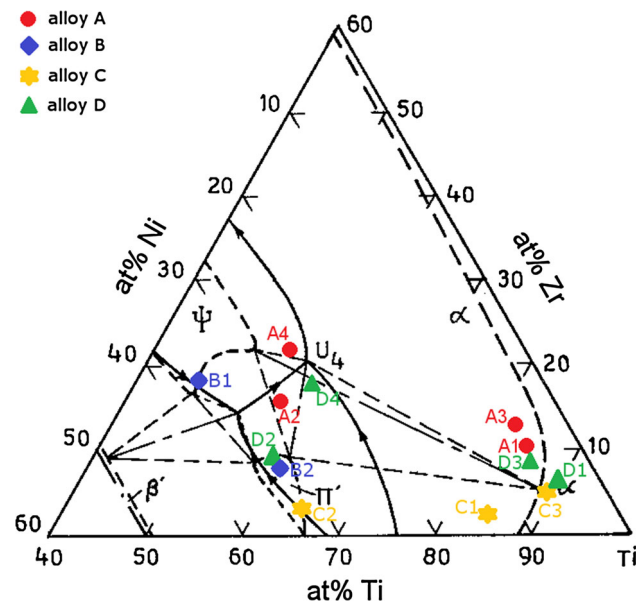
Fig. 5 Ti-rich section of the Ni–Ti–Zr phase diagram (adapted from [11]). The compositions of the phases listed in Table 2 are marked for comparison with the equilibrium phases

Table 4 Mean values of coefficients of thermal expansion in the temperature range from 20 to 700 °C

Alloy	Coefficient of thermal expansion α_T [10^{-6} °C^{-1}]
A (61Ti–20Zr–19Ni)	15.8
C (70Ti–5Zr–25Ni)	13.2
D (64Ti–15Zr–22Ni)	14.0
Al$_2$O$_3$	6.5–8.9 [12]

analysis of the oxygen content was not possible within the spatial and concentration resolution of the available methods.

Thermal expansion coefficient

The coefficient of thermal expansion was determined for each alloy except for alloy B. This alloy seems not to be suitable for joining alumina due to its high contact angle and the missing reaction product at the metal/alumina interface. Table 4 shows the average coefficients of thermal expansion in the temperature range between 20 and 700 °C. The coefficient of thermal expansion for alumina from Ref. [12] is given for comparison.

Discussion

Alloys A, C, and D showed the typical behavior known from reactive wetting: the contact angle of the molten alloy on alumina decreased rapidly at the beginning of the wetting process, and the longer the experiments were

performed, the slower this decrease became. Since it was not possible to identify the exact contact angles while the melting of the alloy was still ongoing, the actual initial contact angles are likely to be higher than depicted in Fig. 3. This problem is discussed in more detail by Meier et al. [13]. They tried to solve the issue by stacking the reactive element on top of the base metal. This way the reactive element is not in contact with the substrate until both components are liquid. Using this method, they still observed spreading of the droplet during the long heating time of about 1 h, but to a much lower extent. This method could not be used in our experiments. To ensure the homogeneity of the alloys, it was necessary to remelt them several times due to the poor mixing of the components. This is a common problem when working with Ni–Ti–Zr alloys [14]. Placing all starting materials separately on the substrate would not have led to a sufficient homogeneity of the alloys. Compared to other known reactive wetting systems (e.g., Ag–Cu–Ti [15, 16]), the equilibrium contact angle was obtained relatively quickly (after 50–100 s). This is likely to be due to the high amount of the reactive elements Ti and Zr in the alloys, which ensured the ongoing reaction at the triple point of the droplets.

Alloy B did not possess the typical characteristics of reactive wetting: the contact angle remained nearly constant during the experiment, and in the SEM analysis no reaction phase was present at the metal/alumina interface. It could be possible that there is a delayed chemical reaction that starts after a first metastable contact angle has formed as suggested by Saiz et al. [5]. Although the annealing temperature was held for another 5 min without any change in the shape of the droplets, it cannot be completely excluded that the holding time was still too short. This alloy was not analyzed any further, as it cannot

Table 3 Properties of the phases found in the cross sections of the wetting samples [11]

Phase designation	Composition	Pearson symbol	Space group	Prototype	Lattice parameters (nm)		
					A	B	C
α (Ti, Zr)	–	hP2	P6$_3$/mmc	Mg	–	–	–
π′	NiTi$_2$	cF96	Fd$\bar{3}$m	CFe$_3$W$_3$	1.1324	–	–
Ψ	NiTiZr	hP12	P6$_3$/mmc	MgZn$_2$	0.5200	–	0.8520

be used as active braze alloy due to the missing chemical reaction.

Alloys A, C, and D showed a phase near the metal/alumina interface that was formed by a chemical reaction with the alumina. This phase could not be assigned to one of the equilibrium phases known in the Ni–Ti–Zr system [11]. Although the presence of oxygen expected in this phase could not be detected with the available analysis methods, the assumption of a chemical reaction is supported by the presence of some aluminum in these phases. Whereas a part of the aluminum content may arise from the alumina due to the excitation volume of the EDX analysis, a comparison with similar measurements of samples of alloy B shows that the excitation volume cannot fully explain the high amount of detected aluminum. The exact composition of the phase at the metal/alumina interface could not be analyzed with the available methods. The problem of identifying the reaction phase is not unusual for reactive wetting. Hosking et al. [17] were analyzing the wetting behavior of different Ag–Ni–Mo–V alloys on alumina. Due to the thin and discontinuous reaction layer, the authors were not able to identify the reaction product with certainty and proposed $AlVO_3$ or AlV_2O_4 as possible phases. Lin et al. [18] investigated the wetting of Cu–Sn–Ti alloys on alumina and detected Cu, Sn, Ti, and O in the reaction layer, but could not identify it any further. Even in the most common system of Ag–Cu–Ti alloys on alumina, different authors identified different reaction products such as Ti_3Cu_3O [16], $Cu_2(AlTi)_4O$ [19], or $Ti_3(Cu,Al)_3O$ [20].

Alloys C and D exhibited a similar microstructure at the metal/alumina interface. In both systems a discontinuous reaction layer with a similar composition was formed. Both reaction layers had a thickness of about 1 μm. It can be assumed that this is the same phase in both alloys, as the observed variation in composition is most likely due to the small size of this phase and the finite excitation volume of the electron beam. The shape and size of the reaction phase was independent of the annealing time, but it cannot be excluded that they still could grow at longer holding times. While the small spatial extension of the reaction phases is problematic for the SEM analysis, it should be advantageous for the mechanical properties of the joint. It is known that these phases are often very brittle. A thin reaction phase minimizes the probability of crack initiation and propagation at the metal/alumina interface.

The microstructure of the samples with alloy A differs significantly from the other alloys. Close to the metal/alumina interface two ($T = 930$ °C) or three ($T = 990$ °C) different phases were present, only at distances >20 μm the microstructure of the bulk alloy was observed. The phase in direct contact to the alumina had a similar composition as the reaction phase observed in the samples of alloy C and D and formed first during the experiment. At temperatures above 980 °C, a layer of a second phase forms adjacent to this first reaction phase. As that phase is not part of the equilibrium phase diagram [11], it is concluded that this phase is also the result of a chemical reaction between the liquid braze alloy and the alumina that occurs only at higher temperatures. Despite not being in direct contact with the alumina, the formation of this additional phase has a positive influence to the wetting behavior and the contact angle decreases by approximately 20°. A possible explanation of this behavior is the formation of the first reaction layer at the beginning of the wetting. On this reaction layer the droplet forms an initial contact angle. The reaction occurs at the beginning of all wetting experiments performed with alloy A, independent of the applied temperature. This explains the similar wetting behavior in the first 10 s of the experiments. When applying temperatures above 980 °C, a second reaction occurs afterward. The droplet then continues spreading on the new reaction phase until the equilibrium contact angle is reached. This explains the lower contact angle observed in the wetting experiments that were performed at temperatures above 980 °C. Between the reaction phases and the microstructure of the bulk alloy, a layer of α (Ti, Zr) phase of ∼15 μm thickness was found. Measurements of the coefficients of thermal expansion of all of the pure phases found in the samples (except the reaction phases) showed that the thermal expansion behavior of the α (Ti, Zr) phase is closest to alumina as compared to the other phases. This layer of α (Ti, Zr) phase could be advantageous for the joint properties as it may lead to lower thermal-induced stresses that arise through cooling the samples to room temperature.

The coefficients of thermal expansion of the alloys A, C, and D are all higher than that of alumina, which causes thermally induced stress upon cooling the samples. However, the most commonly used system for brazing ceramics Ag–Cu–Ti exhibits even higher coefficients of thermal expansion, e.g., the commercially available active braze alloy Ticusil® a value of 18.5×10^{-6} °C^{-1} [21]. The low difference of the thermal expansion coefficients should be advantageous, as it reduces the thermal-induced stresses at the interface.

Summary

The wetting behavior of four ternary Ni–Ti–Zr alloys on alumina with two different purities was analyzed in a high purity Ar-atmosphere. Three of the alloys showed characteristics typical for reactive wetting. The lowest wetting angle of 40° was observed for the alloy 61Ti–20Zr–19Ni at temperatures above 980 °C. A reaction layer of about 1 μm thickness was formed at the metal/alumina interface. This

reaction layer also had a similar composition for all of the three alloys that showed reactive wetting. An additional reaction phase was present at the metal/alumina interface of samples with the lowest contact angle of 40°. The coefficients of thermal expansion of the alloys extended from 13.2 to 15.8×10^{-6} °C^{-1}, which is closer to the value of alumina than the values of other commonly used active braze alloys.

References

1. Nicholas MG (ed) (1990) Joining of ceramics. Chapman and Hall, London

2. Eustathopoulos N (2005) Progress in understanding and modeling reactive wetting of metals on ceramics. Curr Opin Solid State Mater Sci 9(4–5):152–160

3. Eustathopoulos N (1998) Dynamics of wetting in reactive metal ceramic systems. Acta Mater 46(7):2319–2327

4. Saiz E, Tomsia AP (2005) Kinetics of high-temperature spreading. Curr Opin Solid State Mater Sci 9(4–5):167–173

5. Saiz E, Cannon RM, Tomsia AP (2000) Reactive spreading: adsorption, ridging and compound formation. Acta Mater 48(18–19):4449–4462

6. Gomez-Garcia D, Gutierrez-Mora F, Gallardo-Lopez A, Dominguez-Rodriguez A (2007) A general law for liquid metal-onto-ceramic wetting: an electrostatic approach. J Eur Ceram Soc 27(11):3307–3310

7. Akselsen OM (1992) Advances in brazing of ceramics. J Mater Sci 27(8):1989–2000. doi:10.1007/BF01117909

8. Kumar G, Prabhu KN (2007) Review of non-reactive and reactive wetting of liquids on surfaces. Adv Colloid Interface Sci 133(2):61–89

9. Schwartz Mel M (1990) Ceramic joining. ASM International, London

10. Naidich YV, Zhuravlev VS, Gab II, Kostyuk BD, Krasovskyy VP, Adamovskyy AA, Taranets NY (2008) Liquid metal wettability and advanced ceramic brazing. J Eur Ceram Soc 28(4):717–728

11. Gupta KP (1999) The Ni–Ti–Zr system (nickel–titanium–zirconium). J Ph Equilib 20(4):441–448

12. Martienssen W, Warlimont H (2005) Springer handbook of condensed matter and materials data. Springer, Berlin

13. Meier A, Chidambaram PR, Edwards GR (1995) Generation of isothermal spreading data for liquid reactive metals on ceramic substrates: the copper–titanium/alumina system. J Mater Sci 30:3791–3798. doi:10.1007/BF01153936

14. Davis JP, Majzoub EN, Simmons JM, Kelton KF (2000) Ternary phase diagram studies in Ti–Zr–Ni alloys. Mat Sci Eng A 294:104–107

15. Wu M, Cao CZ, Rafi ud din, He XB, XH Qu (2013) Brazing diamond/Cu composite to alumina using reactive Ag–Cu–Ti alloy. Trans Nonferr Met Soc China 23(6):1701–1708

16. Voytovych R, Robaut F, Eustathopoulos N (2006) The relation between wetting and interfacial chemistry in the CuAgTi/alumina system. Acta Mater 54(8):2205–2214

17. Hosking FM et al (2000) Microstructural and mechanical characterization of actively brazed alumina tensile specimens. Weld J Res Suppl 79(8):222–230

18. Lin C, Chen R, Shiue R (2001) A wettability study of Cu/Sn/Ti active braze alloys on alumina. J Mater Sci 36(9):2145–2150. doi:10.1023/A:1017531730604

19. Jasim KM et al (2010) Actively brazed alumina to alumina joints using CuTi, CuZr and eutectic AgCuTi filler alloys. Ceram Int 36(8):2287–2295

20. Shiue RK, Wu SK, O JM, Wang JY (2000) Microstructural evolution at the bonding interface during the early-stage infrared active brazing of alumina. Metall Mater Trans A 31(10):2527–2536

21. Halbig MC, Coddington BP, Asthana R, Singh M (2013) Characterization of silicon carbide joints fabricated using SiC particulate-reinforced Ag–Cu–Ti alloys. Ceram Int 39(4):4151–4162